

Superhydrophobic porous silicon surfaces

M. Balucani*, G. Bolognesi**, C. M. Casciola**, M. Chinappi***, A. Giacomello**, P. Nenzi*

*Sapienza, University of Rome, DIET

Via Eudossiana, 18, 00184 Rome, Italy, balucani@die.uniroma1.it

**Sapienza, University of Rome, DIMA

Via Eudossiana, 18, 00184 Rome, Italy, carlomassimo.casciola@uniroma1.it

***Sapienza, University of Rome, Dip. Scienze Biochimiche

P.le Aldo Moro 5, 00185 Rome, Italy, mauro.chinappi@uniroma1.it

ABSTRACT

In this paper, we present an inexpensive technique to produce superhydrophobic surfaces from porous silicon. Superhydrophobic surfaces are a key technology for their ability to reduce friction losses in microchannels and their self cleaning properties. The morphology of a p-type silicon wafer is modified by an electrochemical wet attack to produce pores with controlled size and distribution and coated with a n-alkylsilane self assembled monolayer. Large contact angles are observed on such surfaces and the results are compared with classical wetting models (Cassie and Wenzel) suggesting a mixed Wenzel-Cassie behaviour. The presented technique represents a cost-effective means for friction reduction in microfluidic applications, such as lab-on-a-chip.

Keywords: macroporous silicon, superhydrophobic surfaces, lab on chip, slip

1 INTRODUCTION

In recent years superhydrophobic surfaces (SHS) [1] have increasingly attracted the interest of the scientific and technological community thanks to their self-cleaning properties and to the large wall-slippage they present for liquid water (slip lengths on the order of micrometers) [2]. Natural SHSs have been observed in some plant leaves (Lotus) and insect wings and are characterized by large contact angles, low contact angle hysteresis and large slippage. The typical feature of natural SHSs is their micro/nano scale roughness where air bubbles can get trapped. The presence of the air-water interface is the cause of the surface's low contact angle hysteresis and slippage. Several research groups have been working towards the development of synthetic SHSs capable of mimicking the roughness hierarchy of natural SHSs. The air-trapping capability of a surface alone is not enough for SHS application to microfluidics. A crucial issue, indeed, is the stability of the Cassie state [3], since trapped bubbles, under environmental fluctuations, could lead to the transition to the Wenzel state, with water filling completely the roughness elements. A strategy to fulfill this requirement is combining surface morphology modification and hydrophobic coating. The Cassie-Wenzel transition threshold is ac-

tually affected by the liquid-solid interface energy which can be significantly reduced by appropriate surface coating, e.g. by n-alkylsilane self assembled monolayers.

A promising approach to produce robust and economical silicon SHSs is the use of porous silicon [4]. Porous silicon (pSi) is made by crystalline silicon (cSi) anodization (electrochemical wet etching) in electrolytes (aqueous or organic) containing HF. The morphology of pSi can be easily controlled and, depending on the process parameters, spans from 2 nm (nanoporous silicon) up to hundreds of nm (macroporous silicon). The wetting properties of porous silicon strictly depend on the surface morphology, in particular on the pore diameter and porosity. Nanoporous silicon is reportedly highly hydrophilic [5], while macroporous silicon, without surface coatings, can be either highly hydrophobic [5], or hydrophilic, as in this work, depending on the electrolyte used in the electrochemical etching. SHSs characterized by contact angles in excess of 150° have been recently obtained from pSi surfaces by morphology modification and/or coating of the surface with a low surface energy layer [5], [6].

In this paper we present an easy-to-implement and economical procedure to realize and characterize macroporous silicon SHSs.

2 EXPERIMENTAL METHODS

2.1 Surface preparation

The sample SHS are realized from 10-20 Ωcm resistivity p-type silicon wafers with {100} orientation. A macroporous silicon layer of 20 μm thickness is obtained by anodization in HF:DMSO (10 : 46) solution at 10 mA/cm² for 30 minutes. During the anodization process, only a circular area of 1 cm² is exposed to the solution. Hence, on the same wafer, both smooth and porous regions are present. Figures 1 and 2 show a top view and a cross section of a representative porous silicon sample obtained with the described process. The macroporous silicon layer is characterized by a porosity of 55% and average pore Feret diameter of $1.72 \pm 0.92 \mu\text{m}$. Porosity is measured from the grayscale top view SEM images, see Fig. 1, by counting the percentage of pixels whose intensity exceeds a set threshold. This figure accounts for the fully developed pores, corresponding to

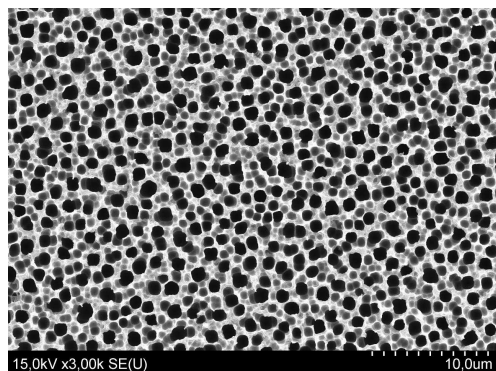


Figure 1: Top view of macro porous silicon sample. Pores appears in black and the grey areas are the inter-pores, pits in the silicon surface that have not reached full depth.

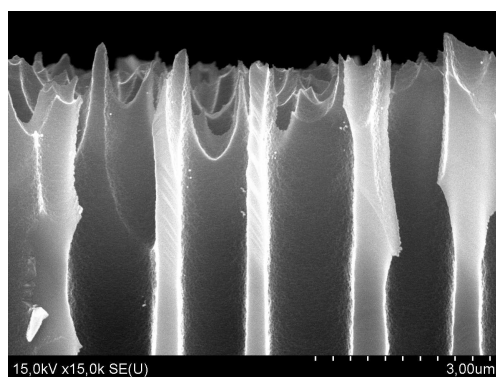


Figure 2: Section of the macroporous silicon layer near the surface. Superficial roughness, due to pore walls dissolution and inter-pores is also evident from this section.

to the darker regions of Fig. 1, as well as the partially developed ones, see Fig. 2 and explanation therein.

The wafers are then coated with perfluoro-octyltrichlorosilane via physical vapour deposition (PVD). We adopt the following procedure. Immediately after anodization the samples are rinsed in DI water and dried in N_2 current. The surface is then activated in oxygen plasma by a Reactive Ion Etching (RIE) process. Finally the samples are coated with a silane layer via low pressure PVD. In addition, the effect of acetone washing on silanized samples is investigated, by performing a 4 min sonication of some samples.

2.2 Contact angle measurement

We adopt the sessile drop method to measure the contact angles (CA) over the porous silicon samples. We use a Nikon D7000 camera, equipped with a Micro-Nikkor 60mm $f2.8/D$ objective, to record images of millimeter size sessile DI water drops, at rest over horizon-

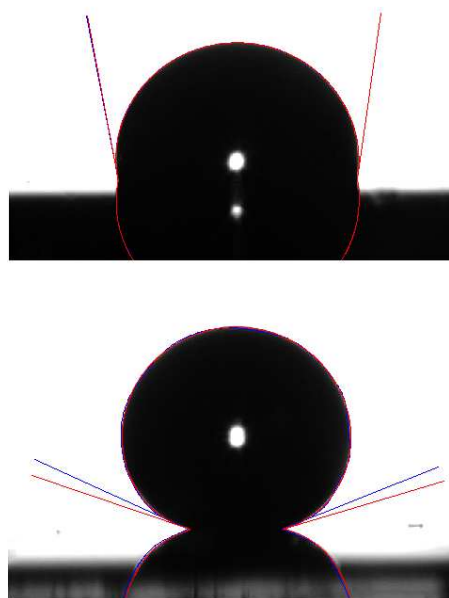


Figure 3: Upper panel: water drop on smooth silicon surface coated with silane (case C in Table 1). Lower panel: water drop on porous silicon surface coated with silane (case A in Table 1). The contact angles are measured using the *DropSnake* plugin for *Imagej*. The blue lines represent the initial guess drop boundary while the red one the final drop profile as calculated by the software.

tal samples. We use a freely available software, *DropSnake* to process images and measure contact angles. In Figure 3 we show some representative results of image analysis. In particular, the top panel shows a sessile drop on a smooth silane coated silicon wafer. The bottom panel, instead, reports a drop on the porous silane coated portion of the wafer. The software requires a user-defined detection of the drop boundary (the blue solid line in the figures), which is used as initial guess for the B-spline fitting of the drop boundary. The red solid line is the final computed boundary whence the left and right contact angles are measured. Further details on the software implementation and accuracy may be found in Ref. [7]. The contact angles extracted with *DropSnake* are found to be robust to small changes in the user-defined definition of the drop boundary.

The average contact angles are reported in Table 1. We compute the averages by analyzing at least 5 images of a sessile drop on the same sample, recorded after moving the drop on different positions of the observed region. In this way we aim at averaging the effect of local morphology on the contact angle, that is one of the causes of contact angle hysteresis. For the same reason, we average right and left contact angles.

Table 1: Summary of the experimental results. Average values between the left and right contact angles are reported. The effect of acetone sonication is also shown.

	Time [min]	Current [mA/cm ²]	Porous	Acetone sonication	Contact Angle (°)
A	30	10	YES	NO	154.5 ± 1.5
B	-	-	NO	NO	98.5 ± 0.6
C	30	10	YES	YES	152.8 ± 1.1
D	-	-	NO	YES	101.8 ± 2.3
E	15	15	YES	NO	160.8 ± 1.6
F	30	5	YES	NO	156.0 ± 1.6

3 RESULTS AND DISCUSSION

In Table 1 we summarize the contact angle measurements under different experimental conditions, with the aim of investigating the effect of (i) surface morphology and (ii) low energy coating. We preliminarily note that non-coated samples are hydrophilic, presenting contact angles of 75° on smooth samples and lower on porous ones. Only contact angles after silanization are reported in Table. 1. Case A refers to silanized porous surfaces obtained by anodization at 10mA/cm² for 30 minutes. The resulting contact angle of 154.5° ± 1.5° shows that the presented method is successful in providing highly hydrophobic silicon surface. The evidence that an effective surface energy modification was prompted by the silane PVD is provided by the contact angle of 98.5° ± 0.6° measured over silanized smooth silicon surfaces (Case B). This value is in line with the experimental contact angle values reported in [8] for surfaces coated with various silane types. This value is also compatible with that reported in the molecular dynamics simulations of [9] for OTS coated cSi. The influence of surface morphology on the contact angle is reflected in the largely different values reported in the cases A and B, and is immediately evident from the images reported in Fig. 3.

The effect of organic solvent washing of the coated samples was tested by performing an acetone sonication of the samples. The cleaning procedure is applied to both porous and smooth silicon surfaces, corresponding to Cases C and D of Table 1, respectively. Even if some benefits are expected from acetone washing, based on what reported in [10], we only detect slight variations in contact angles. A possible explanation of these variations is the effective cleaning from surface contaminants obtained with the acetone wash.

Furthermore, we performed preliminary studies on the sensitivity to process parameters such as density current and time process. We report in Table 1 the contact angle values for samples anodized at 15mA/cm² for 15 minutes (case E) and 5mA/cm² for 30 minutes (case F). In the presented configuration, case E corresponds to the

highest value of current density attainable before electropolishing takes place. From the analysis of SEM sections analogous to Fig. 2, we find that pore morphology shows low sensitivity to current density. Accordingly, anodization parameters affect only weakly the obtained surface water-repellency, see Table 1.

We compare two classical models in order to interpret the reported experimental data in relation to the surface morphology. In particular, the increase of contact angle between the porous silicon and the smooth surfaces is analyzed in view of the Cassie and the Wenzel models.

In the Wenzel model the liquid is assumed to fill in completely the roughness profile. The variation in CA of a rough surface with respect to a perfectly smooth one is ascribed to the larger solid-liquid interface. According to the Wenzel model, the contact angle θ_W is given by

$$\cos \theta_W = r \cos \theta \quad (1)$$

where r is the ratio of the actually wetted area to the projected area of the surface and θ is the contact angle on the smooth surface having the same surface composition.

In the Cassie model air bubbles are trapped within the pores and the liquid is in contact with the solid only at the peaks of the roughness. The resulting contact angle θ_C is

$$\cos \theta_C = -1 + \phi_s(1 + \cos \theta) \quad (2)$$

where ϕ_s is the solid fraction of the interface, i.e. the ratio of solid-liquid area to whole droplet base. Though liquid droplets can be observed in both states, the truly superhydrophobic one is the Cassie state, which, beyond providing a larger CA, promotes water slippage and low CA hysteresis.

Informed by the analysis of the SEM images in section 2.1, it is possible to provide an estimate r and ϕ_s . In particular, ϕ_s coincides with the complement to unity of the surface porosity, that is $1 - \phi_s = 0.45$. The estimate of r is less straightforward. We consider an ideal surface where each pore is perfectly circular and pores are regularly distributed on a periodic square lattice of

size L . In this idealized scheme, we have the following relation between L , ϕ_s and R

$$L^2(1 - \phi_s) = \pi R^2 \quad (3)$$

that, after some manipulations, leads to:

$$r = \phi_s + (1 - \phi_s)(2h/R + 1) \quad (4)$$

This expression is still valid if the pores are not on a regular lattice. However, the formula (4) is not appropriate in the case the pores overlap. Overlaps actually happen as apparent in Fig. 1 and the surface morphology is more complicated of the ideal case we are considering, nevertheless Eq. (4) still provides a rough estimation of r . For $\phi_s = 0.45$ and $h/r \simeq 20$, Eq. (4) yields $r \simeq 27$. This value of r , combined with the average contact angle value measured on smooth silicon computed from Cases B and D in Table 1, that is $\theta = 100^\circ$, leads to a left hand side of Eq. (1) smaller than -1 . While this value has no direct physical meaning, we can note that the closest physically significant case of $\cos \theta_W = -1$ corresponds to the perfectly hydrophobic state, where the surface is not wetted. These considerations suggest that the Wenzel model is not adequate to explain the phenomenology on the considered morphology, and that reasonably the roughness profile is not fully wetted.

The Cassie equation (2), along with the roughness value $\phi_s = 0.45$ and the experimental value $\theta = 100^\circ$, yields $\theta_C \simeq 129^\circ$. The experimental contact angles on porous surfaces coated with silane are however larger than the Cassie estimate, while smaller than the perfectly hydrophobic surface towards which the Wenzel model tends. A possible explanation of the discrepancies between the experimental data and the Wenzel and Cassie models may be found in the partial filling of the pores. This phenomenology is intermediate between the limiting cases of the fully wetted surface and the “fakir” state, embodied by the Wenzel and Cassie models, respectively.

A simple model for this scenario is now presented. Let us suppose that the pores in regular lattice previously introduced, are filled up to a certain depth d . The contact angle is then given by the weighed average of the contact angles, see [1]:

$$\cos \theta^* = \sum_i c_i \cos \theta_i = \phi_s \cos \theta + (r' - 1) \cos \theta - (1 - \phi_s) \quad (5)$$

Here r' has the same expression of Eq. (3), where the wetted depth d is substituted to the pore height h . Substituting in Eq. (5) the experimental data $\theta = 100^\circ$ and $\theta^* = 155^\circ$ we can provide an estimate for the wetted depth $d = 1.25 \mu\text{m}$. This value appears reasonable in view of the SEM images reported in Fig. 2, but provides only a consistency check on the model. Further

investigations of the pore filling of water on hydrophobic rough surfaces is needed to gain a better insight in the phenomenon.

ACKNOWLEDGEMENTS

We would like to thank Prof. G.P. Romano, Prof. L. Marino, and Mr. P.P. Ciottoli for their help and suggestions with the contact angle measurement setup.

REFERENCES

- [1] J. Rothstein, Annual Review of Fluid Mechanics **42**, 89 (2010).
- [2] C. Choi, U. Ulmanella, J. Kim, C. Ho, and C. Kim, Physics of fluids **18**, 087105 (2006).
- [3] A. Cassie and S. Baxter, Transactions of the Faraday Society **40**, 546 (1944).
- [4] V. Lehmann, *Electrochemistry of silicon*, Wiley Online Library, 2002.
- [5] A. Ressine, D. Finnskog, G. Marko-Varga, and T. Laurell, NanoBiotechnology **4**, 18 (2008).
- [6] M. Wang, N. Raghunathan, and B. Ziaie, Langmuir **23**, 2300 (2007).
- [7] A. Stalder, G. Kulik, D. Sage, L. Barbieri, and P. Hoffmann, Colloids and Surfaces A: Physicochemical and Engineering Aspects **286**, 92 (2006).
- [8] D. Janssen, R. De Palma, S. Verlaak, P. Heremans, and W. Dehaen, Thin Solid Films **515**, 1433 (2006).
- [9] M. Chinappi and C. Casciola, Physics of Fluids **22**, 042003 (2010).
- [10] T. Chen and G. Brauer, Journal of Dental Research **61**, 1439 (1982).